

A Multi-domain Magneto Tunnel Junction for Racetrack Nanowire Strips

Prayash Dutta, Albert Lee, Kang L. Wang, Alex K. Jones, and Sanjukta Bhanja

Abstract—Domain-wall memory (DWM) has SRAM class access performance, low energy, high endurance, high density, and CMOS compatibility. Recently, shift reliability and processing-using-memory (PuM) proposals developed a need to count the number of parallel or anti-parallel domains in a portion of the DWM nanowire. In this paper we propose a *multi-domain magneto-tunnel junction (MTJ)* that can detect different resistance levels as a function of a the number of parallel or anti-parallel domains. Using detailed micromagnetic simulation with LLG, we demonstrate the multi-domain MTJ, study the benefit of its macro-size on resilience to process variation and present a macro-model for scaling the size of the multi-domain MTJ. Our results indicate scalability to seven-domains while maintaining a 16.3 mV sense margin.

Index Terms—Spintronic memory, process variation, multi-level cell, macro model

I. INTRODUCTION

DOMAIN-wall memory (DWM), or “Racetrack” memory [1], is among the most promising new memory technologies. As a spintronic memory it inherits the SRAM class access performance and low energy of STT-MRAM with a dramatically higher density (as small as $2F^2$, where F is the technology feature size). Moreover, DWM avoids endurance challenges by providing $\geq 10^{16}$ write cycles [1] compared to endurance limited phase-change and resistive memories at $10^8 - 10^9$ and $10^{11} - 10^{12}$ write cycles, respectively [1], [2].

DWMs are formed from ferromagnetic nanowires. These nanowires extend the magneto-tunnel junction (MTJ) concept of spin-transfer-torque magnetic random access memories (STT-MRAM). DWM nanowires extend the free-layer to store multiple, *e.g.*, 32-512, magnetically polarized domains that correspond to bits, separated by fabricated notches. Between adjacent domains storing complimentary bits, a mobile *domain wall* (DW) that pins to these notches balances the exchange and anisotropic energies [3]. Spin-polarized current can shift the magnetic domains with controlled DW motion.

DWM’s improved density comes at the cost of this data shifting, which is necessary to align data with access points. There has been significant effort on power reduction and speed improvement [1], [4], [5] to optimize DWM shifting overhead and others to address shift reliability [6], [7].

P. Dutta and S. Bhanja are with the Department of Electrical Engineering, University of South Florida, Tampa, FL 33620, USA e-mail: {prayash,bhanja}@usf.edu.

A. Lee and K. L. Wang are with the Department of Electrical and Computer Engineering, University of California at Los Angeles, Los Angeles, CA 90095, USA e-mail: {alee0618,klwang}@ucla.edu.

A. K. Jones is with the Department of Electrical and Computer Engineering, University of Pittsburgh, Pittsburgh, PA 15261, USA email: akjones@pitt.edu

This work was partially funded by NSF CNS-1822085, CNS-2133267, CNS-2133340, NSA, and Laboratory of Physical Sciences .

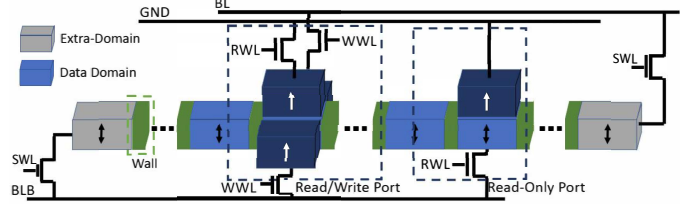


Fig. 1: Anatomy of a DWM nanowire [5].

Transverse read [8] has recently been proposed to count the number of parallel or anti-parallel (*i.e.*, count of ‘1’s) between two access ports of the nanowire. It applies a much smaller than a shifting current, $R_T \ll R_S$ across BLB and GND by opening WWL in Fig. 1 to detect the tunneling magnetoresistance (TMR) of multiple domains against the fixed layer of an MTJ, *e.g.*, the read-only access port shown in dark blue. However, proximity of the domain to the tunneling effect can create variation in the resistance for different permutations of data and limit the scalability of how many domains can be sensed. Furthermore, this structure is likely quite sensitive to process variation. Thus, we propose a *multi-domain magneto tunnel junction* device that can count the number of 1’s in a segment of the nanowire while having the potential for improved scalability and better resiliency to process variation.

II. MULTI-DOMAIN MAGNETO TUNNEL JUNCTION

Our proposed multi-domain MTJ is shown in Fig. 2. The multi-domain MTJ is similar to the read-only access port from Fig. 1 except visualized with the fixed layer and MgO below the free layer and covering multiple domains. The system behaves like k parallel resistors where k is the number of domains covered by the multi-domain MTJ. Each domain’s region forms a high or low resistance state depending on parallel (-Z) or anti-parallel (+Z) magnetic polarization. Thus, the multi-domain MTJ resistance is determined by the number of parallel (or anti-parallel) domains, representing how many, but not which domains store ‘1’s.

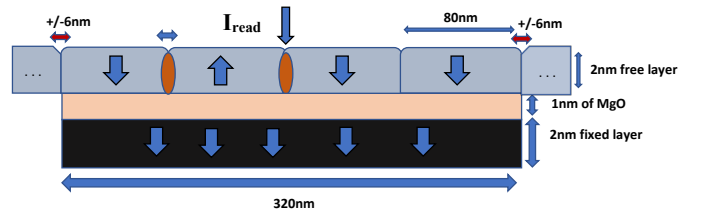


Fig. 2: The structure of the experimental setup. The brown ellipses are the domain walls between two oppositely magnetized domains in the free layer.

TABLE I: Multi-domain MTJ Properties and Dimensions

Property	Values	
Fixed and Free Layer Material	CoFeB	
Fixed and Free Layer Size	320 nm × 40 nm × 2 nm	
Domain Size	80 nm × 40 nm × 2 nm	
Notch dimensions	12 nm × 10 nm × 2 nm	
MgO Layer Size	320 nm × 40 nm × 1 nm	
CoFeB Parameters		
AMR Ratio	0.014	K_u 99 999 erg/cc
Resistivity	15 $\mu\Omega$ cm	M_s 1200 emu/cc
MgO TMR Ratio	0.8	Exchange Stiffness 2.2 μ erg/cm
		J_C 3.21×10^{10} A/m ²

Prior work has used a spintronic nanowire with a flexible DW to store an analog weight for neural network processing [9]. This requires fine control over the DW motion and high precision sense-amplifiers to detect different analog values. While there are some smaller effects which do perturb the resistance levels based on the actual pattern of ‘1’s in the device, our multi-domain MTJ uses notches to ensure domain stability while shifting and functions as digital device. Z-direction current applied evenly across the multi-domain MTJ can induce flow in the $\pm X$ direction to seek lower resistance paths inducing some Anisotropic Magnetoresistance (AMR). Additionally, DW regions have different resistance properties. Thus, domains containing “1010” will have slightly different resistance than than “1100” due to different numbers of DWs.

Because the multi-domain MTJ is much larger than F , we expect variation to only impact the device at the extremities, creating a small amount of under- or over-hang of boundary domain notches, while the internal domains are covered in their entirety. Thus, the impact is less significant than when aligning a single MTJ to a single DWM domain or detecting the resistance with a freely moving DW.

III. EXPERIMENTAL SETUP AND RESULTS

We simulated the multi-layer structure from Fig. 2 using the LLG micromagnetic simulator [10] using CoFeB and MgO with the parameters shown in Table I, where K_u is the uniaxial anisotropy and M_s is the saturation magnetization. Domains were of 80 nm long, 40 nm wide, and 2 nm thick. 4 domains were included in the MTJ with a 1 nm thick MgO layer and 2 nm thick CoFeB fixed layer. Notches of size 12 nm × 10 nm × 2 nm create pinning sites for DWs.

The fixed layer is magnetized in the $-Z$ direction. Each free layer domains can be magnetized in either $\pm Z$. The MgO layer is a non-magnetic tunneling barrier. We assign $+Z$ (anti-parallel, high resistance) as ‘1’ and $-Z$ (parallel, low resistance) as ‘0’. Our read current (I_{read}) has a read current density $J_c = 3.21 \times 10^{10}$ A/m² and remains an order of magnitude lower than the switching current density to minimize the potential of read disturbance [11]. For more than four domains, I_{read} can increase to keep J_c invariant. We attempted to match experimental parameters with prior transverse read work [8].

The resistance is measured from the top of the free layer to the bottom of the fixed layer in the simulator which originates TMR effects from the MTJ and AMR effects from DWs. The impact of domain contents on voltage is shown graphically in blue based on micromagnetic simulation in Fig. 3. We see good similarity of the voltages for all combinations with the same ‘1’s count and the margin between clusters grows

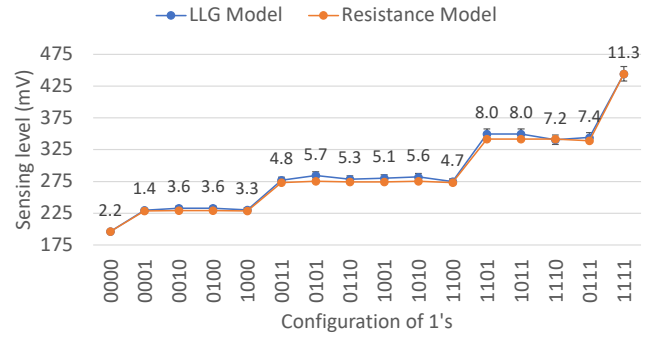


Fig. 3: Sense margin for all permutations of four domains in the free layer. Error bars and labels report 6σ error deviation. as the number of ‘1’s increases. Variability in the cluster is primarily due to the number of DWs. The minimum margin is is 33.5 mV between “0000” and “0001” and the margin grows between groups with more ‘1’s.

To consider process variation we simulated the same model with a 2 nm and 6 nm misalignment between the notch in the extended free layer and the MgO and CoFeB fixed layer (red arrows in Fig. 2), where we treated 5.5 nm as the 6σ in a standard distribution of variation [12]. In this structure, the MgO and CoFeB fixed layer alignment would typically be fabricated with trenches and etching followed by chemical vapor deposition of doped CoFeB and MgO. The alignment concern would come from the location of the notch with the trench wall. The sense margin deviation for 6 nm is shown with error bars to the blue series in Fig. 3. As the error bars are small we also report this deviation in mV as labels. From our read current density, the lowest voltage level that has to be recognized for this resistance gap is still a healthy 28.4 mV which is practical for conventional sense amplifiers [13].

IV. ANALYTICAL MODEL AND SCALING

Detailed magnetic modeling with LLG becomes impractical as number of domains scales. Like prior approaches for analog DW movement in a nanowire [14] and spintronic logic proposals [15], we have constructed a characterized analytical model of the multi-domain MTJ which we describe in Fig. 4. This entire model is a parallel arrangement of some mini-resistive structures. The 4-domain example shown in the figure shows a “0001” but both bordering values are different. Thus, the leftmost domain has a low resistance configuration, denoted R^- for 74 nm and half a DW. The next domain has R^- for 80 nm, followed by R^- for 74 nm, a full DW, and R^+ for 68 nm, with another half DW. From characterization these can be converted to particular resistance values shown in Table II. We can scale to a five-domain MTJ by adding the shaded fixed and barrier layers in Fig. 4 modeling “00010.” The expression replaces the rightmost half DW with a full DW and another R^- for 74 nm. These divisions are segmented by red dotted lines with black lines indicating the borders of the 4-domain and 5-domain examples. “00010” can be calculated through the parallel equivalent resistance to be 431.5 Ω .

We demonstrate accuracy of matching this model to the micromagnetic simulation data for a four domain MTJ in the orange series of Fig. 3, which has an average and maximum error of 1.4% and 3.2%, respectively. We also show data

$$J_C D A_d \left\{ \left(\frac{D-2}{R_{80}^-} + \frac{1}{R_{74}^-} + \frac{1}{R_{68}^+} + \frac{1}{R_{0 \rightarrow 1}^{DW}} + \frac{1}{R_{+Z}^{hDW}} \right)^{-1} - \left(\frac{D-2}{R_{80}^-} + \frac{2}{R_{74}^-} + \frac{2}{R_{-Z}^{hDW}} \right)^{-1} \right\} \quad (1)$$

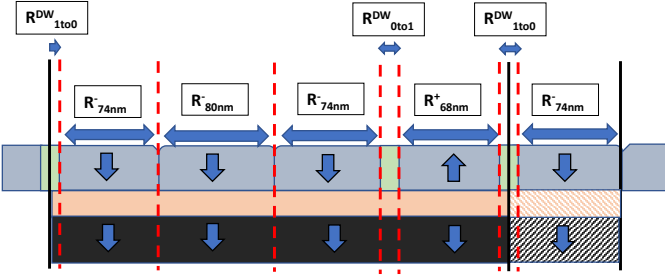


Fig. 4: Resistance modeling of domains in the free layer

TABLE II: Simulation mini structures and resistance

Direction: Size	Notation	Resistance (Ω)
-Z: 80 nm, 74 nm, 68 nm	$R_{80}^-, R_{74}^-, R_{68}^-$	1911, 2048, 2228
+Z: 80 nm, 74 nm, 68 nm	$R_{80}^+, R_{74}^+, R_{68}^+$	4324, 4730, 5143
DW -Z to +Z, +Z to -Z: 12 nm	$R_{0 \rightarrow 1}^{DW}, R_{1 \rightarrow 0}^{DW}$	20053, 20063
Half DW -Z to Z_0 , +Z to Z_0 : 6 nm	$R_{-Z}^{hDW}, R_{+Z}^{hDW}$	35061, 46196

from the five-bit domain model with resistances presented in Table III and sensing margins presented in Fig. 5. We checked data for different numbers of ‘1’s through micromagnetic simulation and determined an average error of $< 1\%$. This data demonstrates six different distinguishable levels when applying the same J_C projects a minimum sense margin is 23.7 mV, which remains detectable by standard sense amplifiers [13]. We can represent the minimum sense margin as described in Eq. 1 where D is the number of domains in the multi-domain MTJ, A_d is the area per domain, and values of R are found in Table II. For six and seven domains, the minimum margin scales to a still detectable 19.3 mV and 16.3 mV, respectively.

V. CONCLUSION

In this paper, we have proposed a brand new technique to count the number of ‘1’s in a DWM nanowire segment. The multi-domain MTJ is sufficiently resistant to effects from process variation. In addition we have presented an analytical model which can be used to explore different configurations of fewer or more domains. In our future work we hope to explore extending the analytical model with impacts from process variation, as well as ways to increase the sense margin.

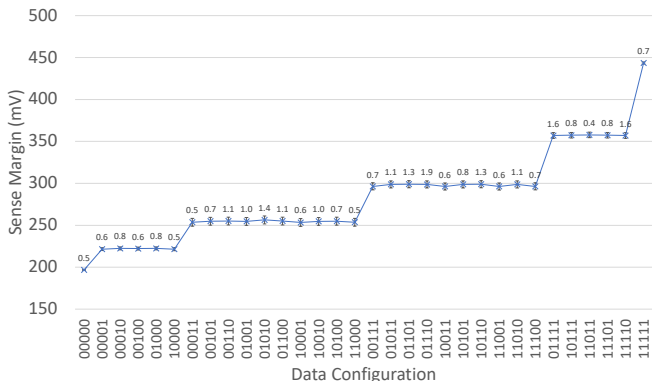


Fig. 5: Modeled 5-domain MTJ, labels report variation due to neighboring domains

TABLE III: Projected Five-domain Resistances

Combination	Resistance	Combination	Resistance
All 0's ↓		Three 1's ↓	
00000	382.10	00111, 11100	576.22
One 1's ↓		01011, 11010	580.11
00001, 10000	431.07	01101, 10110	581.07
00010, 00100, 01000	431.50	01110, 10011, 11001	577.94
Two 1's ↓		10101	583.27
00011, 11000	493.19	Four 1's ↓	
00101, 10100	496.03	01111, 11110	692.87
00110, 01100, 10001	494.45	10111, 11011, 11110	697.39
01001, 10010	495.01	Four 1's ↓	
01010	496.6	11111	864.88

REFERENCES

- [1] R. Bläsing, A. A. Khan, P. C. Filippou, C. Garg, F. Hameed, J. Castrillon, and S. S. P. Parkin, “Magnetic racetrack memory: From physics to the cusp of applications within a decade,” *Proceedings of the IEEE*, vol. 108, no. 8, pp. 1303–1321, 2020.
- [2] J. S. Vetter and S. Mittal, “Opportunities for nonvolatile memory systems in extreme-scale high-performance computing,” *Computing in Science Engineering*, vol. 17, no. 2, pp. 73–82, 2015.
- [3] L. H. Diez and D. Ravelosona, “Controlling magnetism by interface engineering,” in *Magnetic Nano- and Microwires* (M. Vázquez, ed.), Electronic and Optical Materials, ch. 12, pp. 361–379, Duxford, United Kingdom: Woodhead Publishing, 2nd ed., 2020.
- [4] R. Venkatesan, V. Kozhikkottu, C. Augustine, A. Raychowdhury, K. Roy, and A. Raghunathan, “Tapecache: a high density, energy efficient cache based on domain wall memory,” in *Proc. of ISLPED*, pp. 185–190, 2012.
- [5] R. Venkatesan, M. Sharad, K. Roy, and A. Raghunathan, “Dwm-tapestri- an energy efficient all-spin cache using domain wall shift based writes,” in *Proc. of DATE*, pp. 1825–1830, 2013.
- [6] C. Zhang, G. Sun, X. Zhang, W. Zhang, W. Zhao, T. Wang, Y. Liang, Y. Liu, Y. Wang, and J. Shu, “Hi-fi playback: Tolerating position errors in shift operations of racetrack memory,” in *Proc. of ISCA*, 2015.
- [7] S. Ollivier, D. Kline Jr., R. Kawsher, R. Melhem, S. Bhanja, and A. K. Jones, “Leveraging transverse reads to correct alignment faults in domain wall memories,” in *Proc. of DSN*, 2019.
- [8] K. Roxy, S. Ollivier, A. Hoque, S. Longofono, A. K. Jones, and S. Bhanja, “A novel transverse read technique for domain-wall ‘race-track’ memories,” *IEEE TNANO*, vol. 19, pp. 648–652, 2020.
- [9] A. Sengupta, Y. Shim, and K. Roy, “Proposal for an all-spin artificial neural network: Emulating neural and synaptic functionalities through domain wall motion in ferromagnets,” *IEEE TBioCAS*, vol. 10, no. 6, pp. 1152–1160, 2016.
- [10] M. Scheinfein, “Llg micromagnetics simulator,” <http://llgmicro.home.mindspring.com>, vol. 18, p. 25, 1997.
- [11] D. H. Kang and M. Shin, “Critical switching current density of magnetic tunnel junction with shape perpendicular magnetic anisotropy through the combination of spin-transfer and spin-orbit torques,” *Scientific reports*, vol. 11, no. 1, pp. 1–8, 2021.
- [12] M. Komalan, S. Sakhare, T. H. Bao, S. Rao, W. Kim, C. Tenllado, J. I. Gómez, G. S. Kar, A. Furnemont, and F. Catthoor, “Cross-layer design and analysis of a low power, high density stt-mram for embedded systems,” in *Proc. of ISCAS*, pp. 1–4, IEEE, 2017.
- [13] S. Salehi, D. Fan, and R. F. Demara, “Survey of stt-mram cell design strategies: Taxonomy and sense amplifier tradeoffs for resiliency,” *ACM Journal on Emerging Technologies in Computing Systems (JETC)*, vol. 13, no. 3, pp. 1–16, 2017.
- [14] C. Wang, Z. Wang, M. Wang, X. Zhang, Y. Zhang, and W. Zhao, “Compact model of dzyaloshinskii domain wall motion-based mtj for spin neural networks,” *IEEE Transactions on Electron Devices*, vol. 67, no. 6, pp. 2621–2626, 2020.
- [15] X. Hu, A. Timm, W. H. Brigner, J. A. C. Incurvia, and J. S. Friedman, “Spice-only model for spin-transfer torque domain wall mtj logic,” *IEEE Transactions on Electron Devices*, vol. 66, no. 6, pp. 2817–2821, 2019.